

Plant plasma membrane vesicles interaction with keratinocytes reveals their potential as carriers



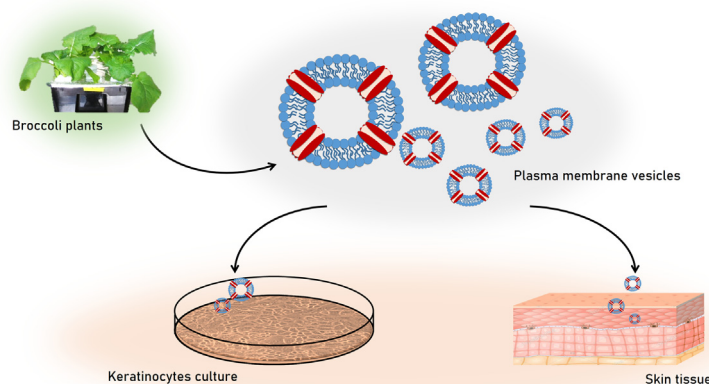
Lucía Yepes-Molina, Maria Carmen Martínez-Ballesta, Micaela Carvajal *

Plant Nutrition Department, Centro de Edafología y Biología Aplicada del Segura (CEBAS-CSIC), Campus de Espinardo, E-30100 Murcia, Spain

HIGHLIGHTS

- Broccoli root vesicles showed stability and high entrapment efficiency.
- Nanoencapsulation with membrane vesicles provide an efficient system for keratinocytes cell delivery.
- Effectivity is probed by penetrating in skin layers.

GRAPHICAL ABSTRACT



ARTICLE INFO

Article history:

Received 9 October 2019
Revised 4 February 2020
Accepted 8 February 2020
Available online 8 February 2020

Keywords:

Broccoli
Encapsulation
Keratinocytes
Nanocarrier
Skin

ABSTRACT

During the last few years, membrane vesicles (as exovesicles) have emerged as potential nanocarriers for therapeutic applications. They are receiving attention due to their proteo-lipid nature, size, biocompatibility and biodegradability. In this work, we investigated the potential use of isolated root plasma membrane vesicles from broccoli plants as nanocarriers. For that, the entrapment efficiency and integrity of the vesicles were determined. Also, the delivery of keratinocytes and penetrability through skin were studied. The results show that the broccoli vesicles had high stability, in relation to their proteins, and high entrapment efficiency. Also, the interaction between the vesicles and keratinocytes was proven by the delivery of an encapsulated fluorescent product into cells and by the detection of plant proteins in the keratinocyte plasma membrane, showing the interactions between the membranes of two species of distinct biological kingdoms. Therefore, these results, together with the capacity of brassica vesicles to cross the skin layers, detected by fluorescent penetration, enable us to propose a type of nanocarrier obtained from natural plant membranes for use in transdermal delivery.

© 2020 THE AUTHORS. Published by Elsevier BV on behalf of Cairo University. This is an open access article under the CC BY-NC-ND license (<http://creativecommons.org/licenses/by-nc-nd/4.0/>).

Introduction

In recent years there has been growing interest in the development of nanocarriers due to their multiple biotechnological applications; for example, in skin therapy and in the cosmetic industry.

Peer review under responsibility of Cairo University.

* Corresponding author at: CEBAS-CSIC, P.O. Box 164, 30100 Espinardo, Murcia, Spain.

E-mail address: mcavajal@cebas.csic.es (M. Carvajal).

<https://doi.org/10.1016/j.jare.2020.02.004>

2090-1232/© 2020 THE AUTHORS. Published by Elsevier BV on behalf of Cairo University.

This is an open access article under the CC BY-NC-ND license (<http://creativecommons.org/licenses/by-nc-nd/4.0/>).

The power of nanocarriers in these areas stems from their potential use as controlled and targeted delivery systems for bioactive compounds or drugs [1]. There are many types of nanocarriers: lipid-based nanocarriers, metallic nanoparticles, simple emulsions, vesicular nanosystems and polymeric nanoparticles [2]. One of the main challenges in therapies and cosmetology is to find biocompatible and biodegradable systems that can be functionalised.

In skin therapies and cosmetics, another important requirement of nanocarriers is that they be skin-permeable. Skin permeability is very important because human skin is a gateway to the body and the target organ of skin therapies. However, the skin layers are not accessible to all molecules. Skin acts as an efficient barrier to molecules exogenous to the body and only allows the entrance of small molecules [3]. This aspect is the main limitation to the use of nanoparticles in cosmetic products and according to the 500 Dalton (Da) rule, for skin penetration by water-soluble chemical compounds and drugs, the skin penetration is limited to a maximum molecular weight of 500 Da [4].

The skin is an organ formed by three layers: epidermis, dermis and hypodermis. The most superficial layer is the stratum corneum (SC), which is part of the epidermis and is formed by 10 to 25 layers of stacked corneocytes, disposed parallel to the skin surface [5]. The SC layers are united by assembled SC lipid bilayers [3]. The SC is the layer that must be overcome, since its main function is to act as an impermeable barrier. Therefore, increased permeation through the SC is essential for percutaneous absorption of cosmetic or therapeutic agents [3]. Below the SC, the viable epidermis contains predominantly (80–90%) keratinocyte cells and is a region where drug binding can occur. The following layer, the dermis, is rich in collagen and the hypodermis, the deepest layer of the skin, is formed of loose connective tissue and fat. However, there is a membrane at the base of the epidermis and also there is recent evidence for the existence of tight junctions in the viable epidermis, both of which may offer resistance to the transport of molecules across the epidermis [6].

Therefore, increased permeation through the SC is essential for percutaneous absorption of cosmetic or therapeutic agents. Nanocarriers have been developed that increase absorption [7], achieving close contact and strong interaction with the most superficial skin layer. Therefore, the main challenge in nanocarrier development is the release of the encapsulated compound without causing damage to the skin that alters its barrier functionality, as occurs with different surfactants and organic solvents [8].

Other important characteristics of skin therapies and cosmetics are their stabilities. The shelf-life required for a cosmetic product is normally two years; therefore, it is essential to study the average life of all the components that are added to the cosmetic products, including nanocarriers. The stability of carriers is complex since it includes not only the stability of each chemical compound but also the physical and biological stability. Therefore, the evaluation of all these parameters will determine potential nano-applications. Nanocarriers are used in cosmetic products to improve penetration of the bioactive compound through the skin, with different purposes: to increase skin hydration, to improve the uniformity of coloured preparations, to prolong fragrance release in perfumes or as natural filters in UV-protection products [9].

Considering all the lipid nanocarriers investigated up until now, together with the development of techniques that allow the manipulation of some of their structural molecules, there are none that possess all the desired characteristics of entrapment, stability, penetrability and release in relation to specific tissue/cell type targeting [10]. In fact, proteoliposomes act as systems of long-term stability [10]. This is due to the lipid-protein environment that is similar to native membranes and allows specific lipid-protein interactions, important for stability [11].

Recently, it was shown that membrane vesicles derived from several natural sources, including plants, are characterised by their biodegradability and biocompatibility, which are due to the similarity of their composition with that of mammalian exosomes [12,13]. This should allow their use as nanocarriers in cosmetics or in therapeutic applications. These vesicles derived from cell membranes are called extracellular vesicles (EVs) [14] and are characterised as one of the main mechanisms of intercellular communication [15].

Vesicles derived from plants have not been deeply assayed for their potential application in skin therapies or cosmetics, but some results have already shown cross-reactions between animal and plant membranes. Thus, Ju *et al.* [12] showed that grape (*Vitis vinifera* L.)-derived exosome-like nanoparticles and mammalian exosomes shared certain proteins (including HSP70 and aquaporins), and lipids enriched in phosphatidic acids and phosphatidylethanolamines. They also had similar nanosize and vesicle structure. The common aspects of these two types of exosome allow grape exosome-like nanoparticles to penetrate within the gut, promote the proliferation of stem cells and help to regenerate intestinal epithelial tissue. Also, mimicry has been found when comparing the cellular processes of plant and animal cells; for example, the release of vesicles as multivesicular bodies (MVBs) into the intercellular space in barley by exocytosis has been related to pathogen defence [16].

This study is focused on the use of plasma membrane vesicles derived from roots of *Brassica oleracea* L. var. *Italica* (broccoli) in biotechnological skin applications. These vesicles are thermodynamically stable [17], have a long shelf-life [18] and are enriched in aquaporins, which have a very important role in the *in vitro* stabilisation of these vesicles [11,19]. In addition, an industrial application of these vesicles would take advantage of surplus broccoli crop biomass since, of the total biomass of this crop, only 25% is marketable in the food industry.

In the present study, we have researched the effect of vesicles extracted from plants, specifically from *B. oleracea*, on skin penetration and delivery. We investigated the entrapment and integrity of the plant plasma membrane vesicles, their fusion with keratinocyte cells and their penetration into porcine skin layers. Different strategies were carried out in order to determine the different properties. For the entrapment, two different dyes were entrapped and measured by spectrophotometry. The fusion of vesicles with keratinocytes was determined by delivering fluorescein diacetate (FDA) from vesicles to cells and was assessed by the increase in the water uptake capacity of keratinocytes and by determination of plasma membrane plant proteins in keratinocytes. Vesicle penetrability through the porcine skin layers was determined by confocal microscopy analysis of the sodium fluorescein (FNA) uptake. Also, the stability of the plant vesicles was determined in a formula cream intended only for experimental use.

Material and methods

Plant culture

Seeds of broccoli were pre-hydrated with de-ionised water and aerated continuously for 24 h. After this, the seeds were germinated in vermiculite in the dark at 28 °C for 2 days. They were then transferred to a controlled environment chamber with a 16 h light and 8 h dark cycle, with temperatures of 25 and 20 °C, and relative humidity of 60 and 80%, respectively. Photosynthetically active radiation (PAR) of 400 $\mu\text{mol m}^{-2} \text{s}^{-1}$ was provided by a combination of fluorescent tubes (Philips TLD 36 W/83, Jena, Germany and SylvaniaF36 W/GRO, Manchester, NH, USA) and metal halide

lamps (OsramHQI, T 400 W, Berlin, Germany). After 5 days, the seedlings were placed in Hoagland nutrient solution with continuously-aerated. After 2 weeks of growth, and after an osmotic shock (12 dS m^{-1}) for 1 week (applied to stimulate the aquaporins synthesis), the roots were harvested for vesicles isolation.

Plant vesicles

The roots were cut into small pieces before vacuum-filtering with a buffer containing 0.5 M sucrose, 1 mM DTT, 50 mM HEPES and 1.37 mM ascorbic acid, at pH 7.5, and supplemented with 0.6% PVP. Each sample was homogenised using a blender and then filtered through a nylon mesh (pore diameter of $100 \mu\text{m}$). The filtrate was centrifuged at $10,000 \times g$ for 30 min, at 4°C . The supernatant was recovered and centrifuged for 35 min at $100,000 \times g$, at 4°C . Then, the resulting pellet was re-suspended in 5 mM potassium phosphate buffer and 0.33 M sucrose, pH 7.8. Plasma membranes were purified from microsomes by partitioning in a two-phase system mixture with a final composition of PEG-3350/Dextran-T500 6.3% (w/w), in the presence of 5 mM KCl, 0.33 M sucrose and 5 mM potassium phosphate buffer (pH 7.8). The system was centrifuged for 5 min at $4000 \times g$. The upper phase was placed in another tube, washed with a solution containing 5 mM phosphate buffer and 0.33 M sucrose, pH 7.8, and centrifuged at $100,000 \times g$ for 35 min. The pellet was re-suspended in 5 mM potassium phosphate buffer and 0.25 M sucrose, pH 6.5. This method of plasma membrane purification provides fractions enriched in plasma membrane with a purity of $\sim 95\%$ [20]. Glycerol was added to the plasma membrane vesicle suspension to give a protein concentration of 1%.

Size of vesicles

The average size of the vesicles and the polydispersity index (PDI) were measured using light-scattering technology, through intensity measurements with a Malvern ZetaSizer Nano XL (Malvern Instruments Ltd., Orsay, France). This equipment has the ability to measure particles with a size range from 1 nm to $3 \mu\text{m}$.

Transmission electron microscopy

The vesicles were pelleted at $100,000 \times g$ and fixed chemically with glutaraldehyde (2.5% in 100 mM phosphate buffer, 2 h at 4°C), osmium tetroxide (1% buffered, 2 h at 4°C) and tannic acid (1% in deionised water, 30 min at 22°C). The pellets were then thoroughly rinsed with water, covered with 2% low-melting-point agarose, dehydrated with ethanol and epoxypropane at 22°C and then embedded in Epon. The blocks were sectioned on a Leica EM UC6 ultramicrotome, collected on Formvar-coated copper grids and stained with uranyl acetate followed by lead citrate. Sections were examined using a JEOL 1011 transmission electron microscope with a GATAN ORIOUS SC200 digital camera. For each sample, 5–10 ultrathin sections were examined.

Vesicles functionality and viability

The functionality and viability of the vesicles were checked by measuring the osmotic water permeability (P_f) by stopped-flow light scattering. The kinetics of the volume adjustment of the membrane vesicles were followed by 90° light scattering at $\lambda_{\text{exc}} = 515 \text{ nm}$. The measurements were carried out at 20°C in a PiStar-180 spectrometer (Applied Photophysics, Leatherhead, UK). The samples were diluted 100-fold in a buffer containing 30 mM KCl and 20 mM Tris-Mes, pH 8.3 ($90 \text{ mOsmol kg}^{-1} \text{ H}_2\text{O}$). The vesicles were then mixed with an equal volume of the same

buffer used for vesicle equilibration but with a sucrose concentration of 540 mM ($630 \text{ mOsmol kg}^{-1} \text{ H}_2\text{O}$). This resulted in a $270 \text{ mOsmol kg}^{-1} \text{ H}_2\text{O}$ inward osmotic gradient. The hypo-osmotic shock associated with membrane dilution induced transient opening of the vesicles and equilibration of their interiors with the extravesicular solution. The P_f was computed from the light-scattering time course, according to the following equation: $P_f = k_{\text{exp}} V_0 / A_v V_w C_{\text{out}}$, where k_{exp} is the fitted exponential rate constant, V_0 is the initial mean vesicle volume, A_v is the mean vesicle surface area, V_w is the molar volume of water and C_{out} is the external osmolarity.

Determination of vesicle entrapment efficiency

Two dyes (fuchsin and bromophenol blue) were used for vesicles entrapment efficiency (EE) studies. For dye encapsulation, $10 \mu\text{l}$ of basic fuchsin (1%, w/v) and $10 \mu\text{l}$ of bromophenol blue (1%, w/v), respectively, were added to 10 ml of vesicles (0.2% protein, w/v). Both mixtures were shaken vigorously and washed in phosphate buffer (0.33 M sucrose, 5 mM potassium phosphate pH 7.8), followed by centrifugation at $100,000 \times g$ for 30 min to remove the dye that was not encapsulated. Absorbance spectra were measured for each dye before and after encapsulation and the maximum absorbance (520 nm, basic fuchsin; 560 nm, bromophenol blue) was taken into account for the quantification of each dye, using standards. To determine the release of dye, samples from the initial encapsulated suspension were centrifuged at $100,000 \times g$ for 30 min and the quantification of each dye was performed by spectrophotometry. This process was repeated 1 month, 2 months and 1 year after dye loading. To determine the EE, the following equation was used:

Where *Total amount* is the total amount of dye used in the preparation and *Amount entrapped* is the dye encapsulated.

Primary normal human epidermal keratinocytes (NHEK) culture

Primary Normal Human Epidermal Keratinocytes (NHEK) from pooled donors, isolated from adult normal human tissues from different locations (face, breast, abdomen and thighs), were purchased from PromoCell (Heidelberg, Germany). Shortly after isolation, all PromoCell NHEK were cryopreserved at passage 2 (P2) using PromoCell's proprietary, serum-free freezing medium, Cryo-SFM. After thawing of the cells by immersion in a water bath (37°C), the cells were transferred to a cell culture vessel containing PromoCell Keratinocyte Growth Medium 2 (KGM2) (bovine pituitary extract 0.004 ml ml^{-1} , epidermal growth factor recombinant human 0.125 ng ml^{-1} , insulin recombinant human $5 \mu\text{g ml}^{-1}$, hydrocortisone $0.33 \mu\text{g ml}^{-1}$, epinephrine $0.39 \mu\text{g ml}^{-1}$, transferrin holo human $10 \mu\text{g ml}^{-1}$, CaCl_2 0.06 mM) pre-warmed to 37°C for 30 min. The cells were incubated in a humidified incubator at 37°C with 5% CO_2 . The medium was replaced after 10–24 h. The subcultures were carried out when cells reached 70–90% confluency. For subculture, the cells were washed with HEPES-BSS solution (HEPES-buffered balanced salt solution) (30 mM HEPES, D-glucose, NaCl, KCl, Na-phosphate and phenol red) and detached with a trypsin/EDTA (0.04%/0.03%) solution. After the cells were detached, the trypsin was neutralised with TNS (trypsin neutralisation solution) (0.05% trypsin inhibitor from soybean and 0.1% BSA). The cell suspension was centrifuged for 3 min at $220 \times g$. The resulting pellet was resuspended in KGM2, and the cells were placed in new cell culture vessels containing KGM2 pre-warmed to 37°C . The vessels were placed in a humidified incubator at 37°C with 5% CO_2 until the cells reached 90% confluency.

Keratinocyte swelling assay

One microlitre of vesicles was added to the cell culture media containing keratinocytes at the confluency stage, to give a final concentration of $0.2 \mu\text{g} \mu\text{l}^{-1}$. After 30 min the same amount of water as was present in the culture media (1 ml) was added to the cell culture to reduce the osmotic potential of the medium. Changes in the cell surface area were followed using a digital camera coupled to an optical microscope (Nikon Eclipse TE2000-U, Nikon Instruments Europe B.V. Amsterdam, The Netherlands), to obtain one image every 5 s. Calculations of the cell surface area, to determine the swelling of the cells, were carried out using ImageJ (Wayne Rasband, National Institutes of Health, USA). Measurements of the osmolarity of the medium were carried out using an osmometer (Digital Osmometer, Roebbling, Berlin, Germany), which provided values of $337 \text{ mOsmol kg}^{-1}$ before water dilution. The assay was also carried out adding only water to reduce the osmolarity of the NHEK medium, as a reference to study the vesicle effect on NHEK.

NHEK membrane extraction and membrane protein identification

Membrane protein identification was carried out after vesicle addition to NHEK in order to determine the presence of plant plasma membrane proteins in NHEK membranes. Vesicles were added to the cell culture medium to give a final concentration of $0.2 \mu\text{g} \mu\text{l}^{-1}$. After 30 min of incubation, the NHEK layer was rinsed twice with culture buffer. The cells were collected with a spatula and the plasma membrane was extracted following the procedure of the ReadyPrep™ protein extraction kit (membrane I), (Bio-Rad, cat. #163-2088, USA). Samples of plasma membranes were digested following the standard procedure for protein identification by LC-MS/MS [20], formed by an Agilent 1290 Infinity II column (Agilent Technologies, CA, USA) connected to a mass spectrometer (Agilent Q-TOF 6550) equipped with an Agilent Jet Stream Dual electrospray (Agilent Technologies, CA, USA). The MS/MS search was performed against the NCBI nr and SwissProt databases.

Study of fluorescein diacetate delivery from vesicles

Fluorescein diacetate (48 mM) (Sigma Aldrich, Spain) was encapsulated in vesicles (0.2% protein, w/v). For the encapsulation, FDA was added to vesicles, shaken vigorously and washed in phosphate buffer (0.33 M sucrose, 5 mM potassium phosphate (pH 7.8)) by centrifugation at $100,000 \times g$ for 35 min. Cells (5000 per cm^2) were exposed to vesicles with FDA encapsulated for 45 min. The cell culture medium was then removed and the cells were washed with PBS. A fluorescence microscope (Nikon Eclipse TE2000-U, Nikon Instruments Europe B.V. Amsterdam, Netherlands) equipped with a digital camera was used to measure FDA fluorescence in the NHEK culture. Excitation of the sample was carried out with 480 nm blue light, and green fluorescence was obtained at 515 nm.

In vitro skin penetration by vesicles

Skin tissue was obtained from the unboiled backs of Landrace Large White pigs (weighing 30–40 kg) from the Department of Cardiology of Hospital Clinic (Universitat de Barcelona, Spain). The skin was dermatomed to a thickness of about $500 \pm 50 \mu\text{m}$ (Dermatome GA630, Aesculap, Tuttlingen, Germany). Then, full skin containing dermis, epidermis and SC was used to perform the experiments.

Skin discs with an inner diameter of 2.5 cm were prepared and fitted into Franz-type diffusion cells. The receptor fluid used to keep the skin moisturised was a phosphate buffered saline (Sigma

P3744). The formulations applied were a) 200 μl of FNA (fluorescein, sodium salt) ($50 \mu\text{g ml}^{-1}$) (Sigma Aldrich, Spain), b) 200 μl of vesicles (0.02% protein, w/v) with FNA ($50 \mu\text{g ml}^{-1}$), encapsulated. For the encapsulation, FNA was added to vesicles, shaken vigorously and washed with phosphate buffer (0.33 M sucrose, 5 mM potassium phosphate (pH 7.8)) by centrifugation at $100,000 \times g$ for 35 min. The cells were placed in a 37°C water bath to ensure that the skin surface was maintained at $32 \pm 1^\circ\text{C}$, to mimic physiological skin temperature. Each formulation was prepared 6 times. The exposure time was 24 h. After the exposure time, the skin surface was washed once with 0.5% lauryl-ether-sulphate and once with 500 μl of ultrapure H_2O , two times.

Whole-skin samples were extracted from the Franz cells and examined with an inverted confocal laser scanning microscope (CLSM) (LEICA TCS-SP2, Leica Microsystems, Wetzlar, Germany) equipped with an ultraviolet/visible light laser. FNA was excited at 460 nm and detected at 515 nm. Whole-skin images were taken to have a 3D reconstruction from the surface to the dermis.

Vesicle stability in a formulation

Vesicle suspensions (0.2% protein, w/v) were mixed with a formula cream (PROVITAL GROUP, Barcelona, Spain –for experimental use only) at 5% (w/w). The cream was prepared so that an aqueous solution could be included without affecting the consistency and feel of the cosmetic preparation. The cream formulation was water, 4% hydroxypropyl starch phosphate, 1.2% xanthan gum, 0.4% glyceryl caprylate, 0.35% glyceryl undecylenate, 0.2% sodium benzoate, 0.2% potassium benzoate and 0.13% citric acid, pH 5.0. The concentration of protein in the mixture was assayed by the Bradford method after washing with phosphate buffer (5 mM potassium phosphate, 0.33 M sucrose, pH 7.8) by centrifugation at $100,000 \times g$ for 30 min, to ensure precipitation of integral vesicles. To check the viability of the vesicles, P_f was measured by stopped-flow light scattering in the same way as for the characterisation of the vesicles. These measurements were also carried out 24 h, 1 month and 1 year later.

Data analysis

The statistical analyses were carried out using R version 3.4.3. The student's *t*-test at $P < 0.05$ was chosen to determine significant differences, between the total amount and the amount entrapped (Fig. 2a) and between time 0 and 1 year (Fig. 6b). Tukey's HSD test at $P < 0.05$ was used to determine significant differences between groups (different times: time 0, 24 h, 1 month and 1 year) in Fig. 6c.

Results

Vesicles characterisation

The vesicles were characterised previously with regard to their chemical composition, stability and integrity [19]. In this work, the size and PDI were measured. The results show that the vesicles had a mean diameter of 361.28 nm and a mean PDI of 0.29 (Table S1).

The morphology of the vesicles was determined by transmission electron microscopy. The images obtained (Fig. 1) show that the vesicles had a consistent spherical morphology.

Encapsulation of dyes

Basic fuchsin and bromophenol blue were encapsulated in broccoli vesicles. The EE of the vesicular systems was 56.12% for basic fuchsin and 42.58% for bromophenol blue (Fig. 2a). To determine the integrity of the vesicles and the competence of the vesicles

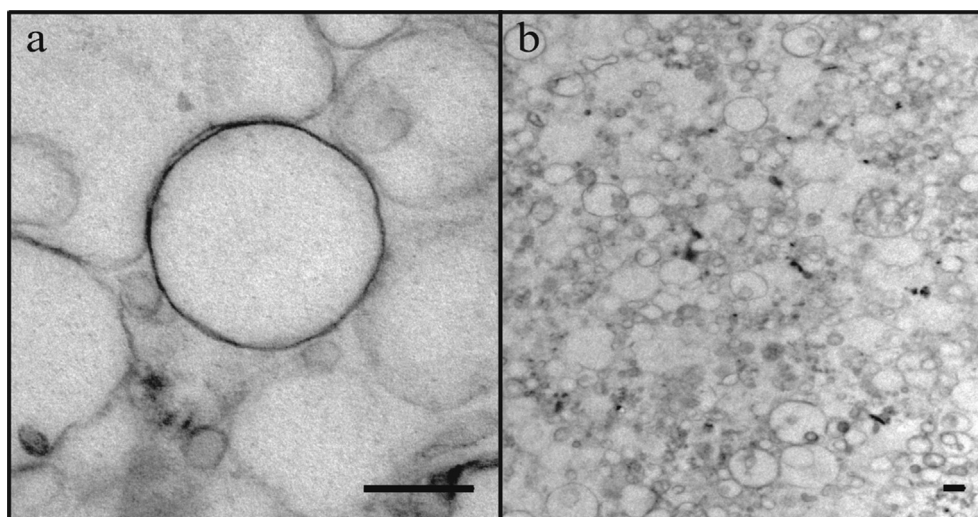


Fig. 1. Transmission electron microscopy images of plasma membrane vesicles from broccoli roots. Scale bar = 200 nm.

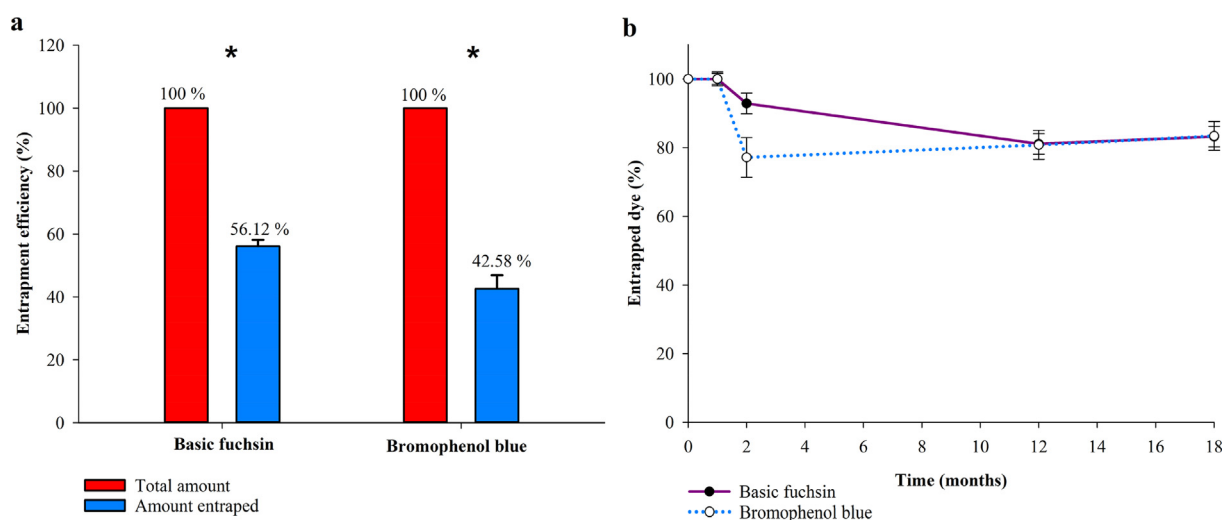


Fig. 2. (a) Entrapment efficiency of basic fuchsin and bromophenol blue in the vesicles and (b) time course (months) of the amount of entrapped dye. Data are means \pm SE ($n = 5$, $n =$ individual vesicles extraction with individual entrapment assay). Asterisk (*) indicates significant differences ($P < 0.05$, student's t -test for paired samples). (For interpretation of the references to colour in this figure legend, the reader is referred to the web version of this article.)

for compound loading, the amount of dye entrapped was measured 1 month, 2 months and 1 year after encapsulation (Fig. 2b). The vesicles were stabilised with a polyalcohol protector (glycerol) during the storage period, as it decreases the surface tension of water [21]. For analysis, the vesicles were washed and precipitated to remove the excess dye that had been released, and the absorbance (λ) was measured for each dye. We found that the percentage encapsulation of basic fuchsin was 100% after 1 month, decreased to 92% after 2 months and was about 80% after 1 year. The bromophenol blue was also maintained at 100% after 1 month, but decreased to 80% after 2 months and remained stable at that value after 1 year.

Fusion of vesicles and keratinocytes

Cell swelling

The swelling of the cells after the addition of the vesicles was determined in order to check if the incorporation of the vesicles into the cells enhanced the water uptake capacity of the keratinocytes. Fig. 3 shows the percentage of cell swelling, based on

the cellular area, induced by reducing the osmolarity of the NHEK culture media. When the NHEK culture was exposed to 1 μ l of vesicles for 30 min and 1 ml of water was added, we found an increment in the cell surface area of about 120% after 60 s. This surface area was maintained until 900 s. Two different phases were observed during the 60 s after the addition of 1 ml of water. The velocity of increase in the surface area was higher during the first 10 s and lower from 20 to 60 s. Regarding the control, for which only water was added to the medium (firstly 1 μ l and, after 30 min, 1 ml more), the percentage of cell swelling reached after 60 s was 12.41% and this remained stable during the rest of the 900 s of measurement.

Plasma membrane proteins identified in the NHEK culture after incubation with broccoli vesicles

Table 1 shows the plasma membrane proteins identified in the NHEK culture after incubation with broccoli vesicles for 30 min. The peptides derived after trypsin digestion of plasma membrane proteins were analysed by LC-MS/MS. Two aquaporins from *Brassica* were found after NCBI and SwissProt database searches, specif-

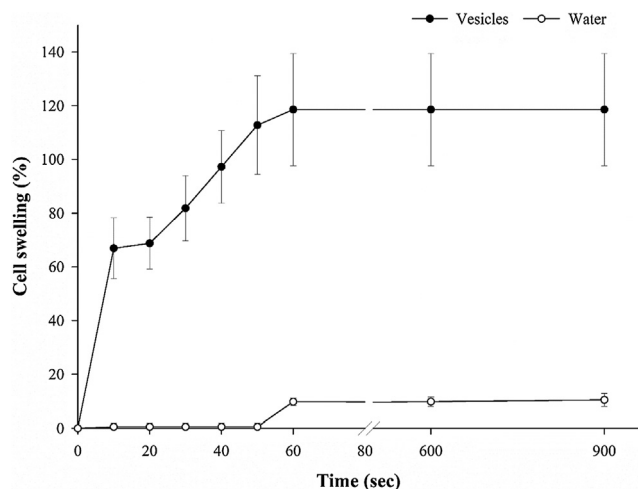


Fig. 3. Cell swelling (%) over time when adding 1 ml of water after the NHEK were exposed for 30 min to 1 μ l of vesicles and 1 μ l of water. Data are means \pm SE (n = 25, n = individual cell measurement).

ically PIP2-4 (plasma membrane intrinsic proteins) and NIP4-2 (NOD26-like intrinsic proteins). These belong to two subfamilies of aquaporins that have been found in the plasma membrane of *Brassica oleracea* and *Arabidopsis thaliana* [20]. In addition, other plasma membrane proteins were found, specifically two phosphatidylinositol phosphate kinases [22].

Fusion of fluorescein diacetate (FDA)-loaded vesicles with primary normal human keratinocytes (NHEK)

Another assay based on a fluorescent dye was carried out to determine the interaction between the vesicles and the NHEK. FDA is a cell-permeant esterase substrate that has been used classically to measure cell viability since, for fluorescence emission to occur, cytoplasmic esterases and cell-membrane integrity are required [23]. The fluorescence (fluorescein) only appears upon hydrolysis by the esterases. In our experiment, the FDA was encapsulated in the broccoli vesicles and added to NHEK. After 30 min, the cell culture was observed under the fluorescence microscope to determine the delivery of FDA from the vesicles into the human cell lines (Fig. 4). Fluorescence appeared in the cells following application of FDA, with encapsulation in vesicles (Fig. 4a). FDA applied without vesicles showed high fluorescence in cells (Fig. 4b). Vesicles without FDA were also applied and used as a negative control (Fig. 4c). Culture cells as seen using light microscopy are also shown (Fig. 4d).

In vitro skin penetration

The two liquid formulations (FNA diluted in water and FNA encapsulated in broccoli vesicles) were applied to the surface of skin that was mounted in Franz cells. Fig. 5 shows 3D reconstructions of the images obtained through CLSM of the distribution and the penetrability of FNA in whole skin after incubation of the two

formulations for 24 h. When FNA in water was applied to the skin surface (Fig. 5a) and incubated, no FNA fluorescence was detected in the deeper layers of the skin. Fluorescence of FNA only appeared in the most superficial layers. Nevertheless, vesicles with encapsulated FNA were distributed and penetrated through different layers, and green fluorescence of FNA was observed to a greater depth (Fig. 5b). In our model we estimated a correlation between *in vivo* and *in vitro* penetration since the determination of FNA in the deeper skin layers *in vitro* can be extrapolated to higher values *in vivo* [24]. Therefore, the *in vitro* experiments provide information concerning the relative permeability.

Stability of the vesicles in a cosmetic

The stability and viability of broccoli vesicles in a cosmetic were evaluated by the osmotic permeability (P_f) of the vesicles and by the amount of protein recovered from the cosmetic. Fig. 6a shows the shrinking kinetics of broccoli vesicles in hyperosmotic conditions at the beginning and end of the experiment. The shrinking kinetics at the two times were similar, with a time-dependent increase in light scattering intensity that was complete in 0.5–1 s for two samples. With the osmotic shrinking kinetics and the volume-to-surface ratio (data not shown), P_f values were calculated. Fig. 6b shows that the P_f values of broccoli vesicles at the beginning and end of the experiment were not significantly different. Fig. 6c shows the lifetime of proteins originally from vesicles that were imbibed in the cosmetic over 1 year. The amount of protein decreased with time, but after 1 year 26.6% decrease from the initial protein content was found in the cosmetic. The amount of protein decreased quickly during the first month, but after this time it remained stable until the last measurement. The transmission electron microscopy image of broccoli vesicles obtained from the cosmetic (Fig. 6d) shows an average size that was similar to that of the initial vesicles.

Discussion

Due to their biocompatibility and biodegradability, materials from plants have been used to prepare nanoparticles with different uses in therapy and cosmetics. Thus, various types of hydrophobic plant compounds have been prepared for encapsulation of bioactive molecules [25]. Also, exosomes from plants such as grapes have been identified as transporters for human tissues [12]. However, the suitability of a nanoparticle for drug delivery requires studies of the drug entrapment, stability, suitability as a carrier and the delivery and penetrability that have not been elucidated yet. Therefore, in this work we studied the potential use of broccoli root plasma membrane vesicles as a nanocarrier for transdermal applications.

Our system is based on vesicles derived from the plasma membrane extracted from broccoli roots. The preparation of the vesicles consists of the purification of plasma membrane using the two-phase aqueous polymer technique [18,26], which allows a reproducible preparation of vesicles in terms of yield and size [11,17,19,20]. In our work, the morphology and physico-chemical

Table 1
Identification of Brassica proteins in plasma membrane isolated from NHEK cells. Proteins identification in NHEK plasma membrane after a database search focused on Brassica plants, where AAs is the number of amino acids, coverage the percentage of the protein sequence covered by identified peptides and peptides the number of distinct peptide sequences in the protein group.

NCBI accession	AAs	MW (Da)	Description	Coverage	Species	Peptides
XP_009131906	285	30118.1	Probable aquaporin PIP2-4 (predicted)	8	<i>Brassica rapa</i>	1
XP_009104033	776	88843.5	Phosphatidylinositol 4-phosphate 5-kinase 4 (predicted)	3	<i>Brassica rapa</i>	1
XP_009148428	759	85962.4	Phosphatidylinositol 4-phosphate 5-kinase 7 isoform X2 (predicted)	2	<i>Brassica rapa</i>	1
XP_013589246	278	29677.3	Probable aquaporin NIP4-2 (predicted)	8	<i>Brassica oleracea</i> var. <i>oleracea</i>	1
CDX76709	1270	141404.8	BnaC08g32950D	1	<i>Brassica napus</i>	1

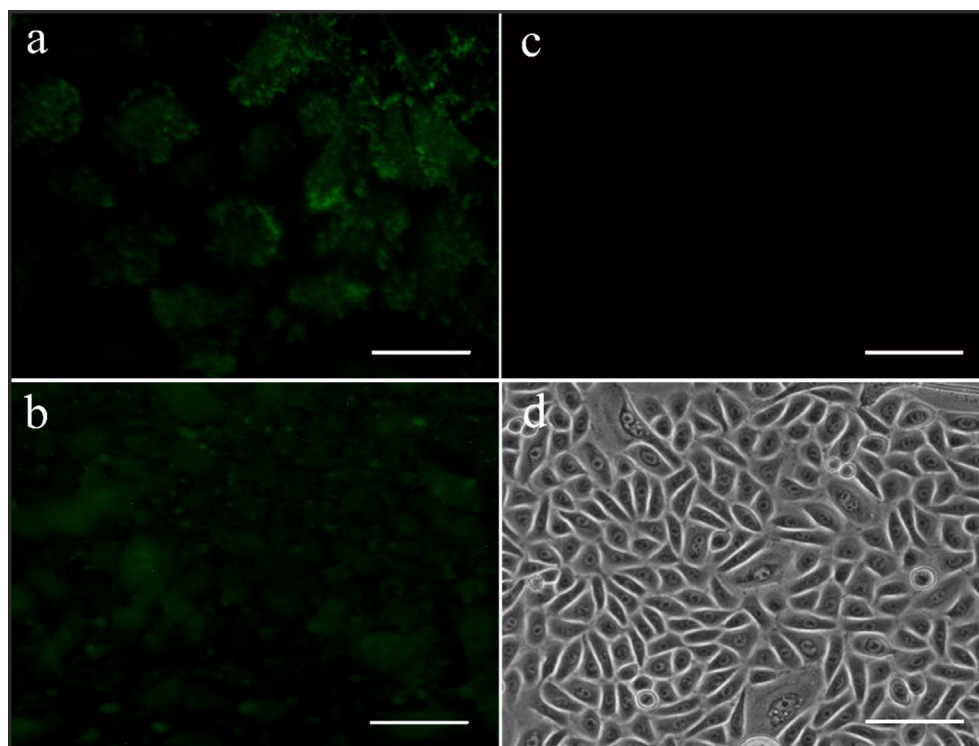


Fig. 4. Delivery of FDA in NHEK. Fluorescence microscopy from NHEK culture after incubation with FDA encapsulated in vesicles from broccoli (a), with free FDA (positive control) (b) and with vesicles without FDA (negative control) (c). Phase contrast microscopy of NHEK culture (d). Scale bar = 100 μm .

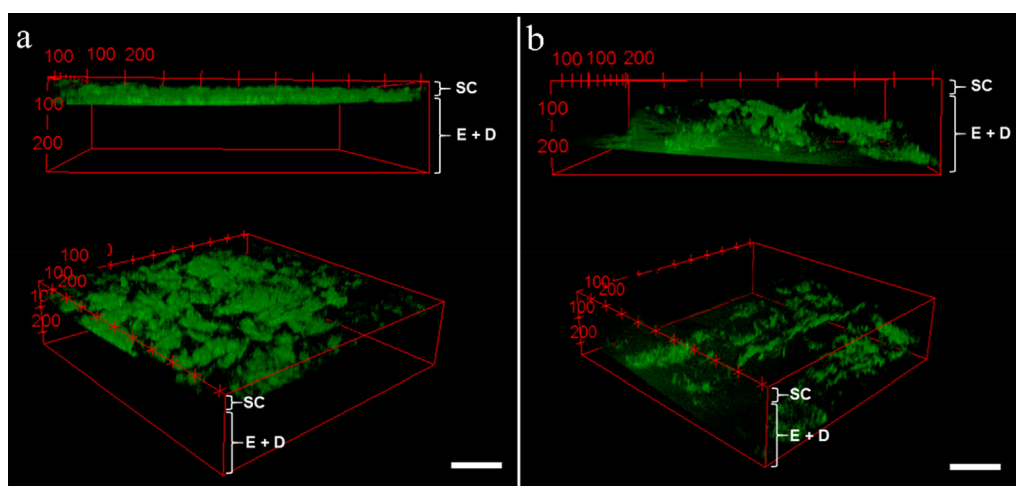


Fig. 5. Penetrability of FNA in whole porcine skin. 3D reconstruction of images obtained through CLSM of whole porcine skin after time incubation with $50 \mu\text{g ml}^{-1}$ FNA in water (a) and with $50 \mu\text{g ml}^{-1}$ FNA encapsulated in broccoli vesicles (b). **Abbreviations:** SC, stratum corneum; E, epidermis; D, dermis. Scale bar = 200 μm .

properties of the vesicles, determined previously [17], make our system suitable for the production of broccoli plant vesicles and their use as nanocarriers [27]. In fact, they are lipoprotein vesicles with a spherical morphology, a diameter of around 400 nm and a PDI of 0.3. It has been reported that the mechanisms involved in transdermal drug delivery depend on the formulation of nanocarriers; in particular, that lipid vesicles with a diameter of 600 nm or above are not able to deliver the encapsulated material into deeper layers of the skin [27]. Therefore, the chemical composition and the diameter of our vesicles will allow their penetration through skin layers.

The EE of the nanocarrier will depend on the integrity and chemical composition [27]. In previous work, it was reported that

plasma membrane vesicles from leaf and root tissues of broccoli plants may be considered as carriers whose stabilisation could be related to aquaporins [11]. However, the EE was not determined. The results obtained in this new work demonstrate that the EE remained at 100% for a short time (1 or 2 months). Also, up to 80% of the test compounds remained in the vesicles after 1 year. Although there is limited information on changes in EE with time, recent results with extract from *Sambucus ebulus* plant loaded into liposomes, transfersomes, and ethosomes showed 75–85% EE for three months at 4 °C [28]. In our experiments, fuchsin is a hydrophilic dye that has been used classically to stain charged molecules and structures such as nucleic acids and the cell wall [29]. Therefore, no interaction with plasma membrane functional groups

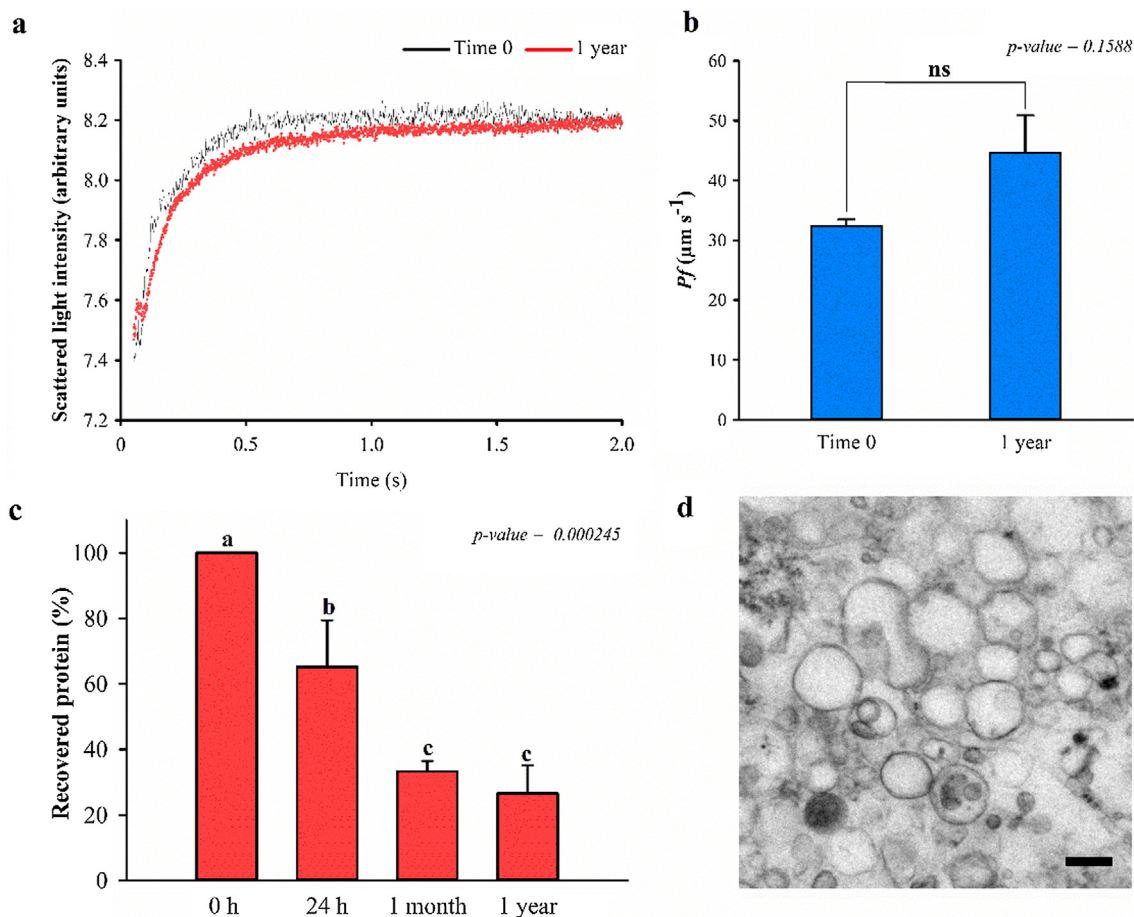


Fig. 6. Stability of vesicles in the cosmetic. Time course of increased scattered light intensity in broccoli vesicles that were washed from the cosmetic (time 0, black; after 1 year, red) and introduced in a stopped-flow apparatus; for both types of membrane preparation, a typical experiment with the average trace of five individual shots and the fitted monoexponential function are shown (a). Osmotic water permeability (P_f , $\mu\text{m s}^{-1}$) of broccoli vesicles at time 0 and 1 year in the cosmetic, after a wash; ns indicates no difference ($P > 0.05$, student's-*t* test for paired-samples) between samples (b). Amount of protein (mg) recovered from cosmetic after a wash at time 0, 24 h, 1 month and 1 year. Different letters represent significant differences according to one-way ANOVA and a posterior Tukey-HSD test ($P < 0.05$) (c). Transmission electron microscopy image of broccoli vesicles obtained from the cosmetic (after 1 year). Scale bar = 200 nm (d). Data in b and c are means \pm SE ($n = 5$). (For interpretation of the references to colour in this figure legend, the reader is referred to the web version of this article.)

has been described. Bromophenol blue was reported to act as a protein-binding dye only at acid pH when organic solvents were added [30]. These dyes (basic fuchsin $323.82 \text{ g mol}^{-1}$ and bromophenol, $669.96 \text{ g mol}^{-1}$) that were used to test EE in our vesicles have in addition a molecular weight similar to some bioactive compounds, such as curcumin ($368.38 \text{ g mol}^{-1}$) or glucoraphanin ($437.49 \text{ g mol}^{-1}$), which are of biotechnological interest for encapsulation [11]. In other results, high or low EE has been attributed to vesicle liposomal size, where larger liposomes (larger than 400 nm) had lower griseofulvin bioavailability than smaller ones [31]. However, a further size reduction of griseofulvin-loaded liposomes ($\leq 400 \text{ nm}$) did not promote higher uptake or bioavailability of griseofulvin. Thus, the particle size of our vesicles, with a z-average size of 361 nm, resulted suitable for dye encapsulation. Also, the particle size of lipidic vesicles has a significant influence on drug penetrability into the skin and vesicles ranging from 10 to 600 nm have been applied in transdermal routes of drug delivery [27].

Also, the solubility of the dyes may condition a slow incorporation into the vesicles and therefore low EE [25]. It has been shown that the EE of lipophilic ibuprofen and ketoprofen in purified egg yolk lecithin liposomes was increased when cargo molecules were octanol/water phase partitioned [32]. Furthermore, beside the fact that our experiments showed an acceptable EE, the results indicate the capacity of the vesicles for long-term encapsulation (1 year).

Our vesicles and other vesicles from natural sources (exosomes from mammalian cells, plant-derived edible nanoparticles) have advantages compared with synthetic nanoparticles that could compensate for a lower EE: on the one hand, each component of synthetic nanoparticles has to be tested in order to determine its toxicity *in vivo*, and on the other hand, the production scale of these vesicles is limited [33]. Our vesicles were obtained as a by-product of broccoli crops, providing a profit advantage in their acquisition. Furthermore, the characterised vesicles were enriched in aquaporins [11], providing a high structural stability [17] and an elevated number of binding domains with certain compounds, such as glucosinolates [11].

An efficient method of delivery into living cells is still a major challenge for nanocarriers. In our experiments, we investigated the fusion ability of the nanocarriers, broccoli vesicles, with keratinocyte human cell lines and followed the swelling rate of the keratinocytes after vesicle incorporation. In addition, the fluorescence signal of FDA after its incorporation in the vesicles and later fusion of the vesicle-FDA system with keratinocytes was assayed for fusion and delivery studies. The cell swelling when the keratinocyte culture was incubated with the broccoli vesicles was much greater than when the vesicles were not present in the culture. These results may be an indication that the cell swelling is a consequence of the high fusion percentage between the broccoli vesicles and the cells. Our vesicles are rich in aquaporins, which

are transmembrane proteins that constitute water channels [19], and these proteins favour the transport of water into the cells due to osmotic changes induced when water is added to the keratinocytes. These results indicate that the broccoli vesicles are, in some way, inducing permeability of the plasma membrane of the keratinocytes.

In the same way, fluorescent keratinocytes imply the delivery of FDA into cells, since this compound only emits fluorescence when an intracellular esterase releases the fluorescein ester [34]. On the contrary, FDA would not come into contact with intracellular esterases and fluorescence would not be visible. In other reports, fusion between liposomes and the plasma membrane of live cells using lipopeptide-modified liposomes has been demonstrated [35]. Therefore, we can assume that the fusion between our broccoli vesicles and keratinocytes occurred. It has been reported that the hetero-fusion could be favoured by the identity among several proteins and the lipid enrichment of plant and animal exosomes [12]. In this work, the authors showed that nanoparticles similar to exosomes derived from grape and exosomes derived from mammalian cells share the HSP70 protein and some aquaporins. Also, the lipid composition regarding phosphatidic acid and phosphatidylethanolamine were similar. In a similar way, Mu *et al.* [36] suggested an interspecies communication mediated by exosome-like nanoparticles derived from plants (grape; grapefruit, *Citrus × paradise*, M.; ginger, *Zingiber officinale*, R.; and carrot, *Daucus carota* subsp. *sativus*), which induced the expression of crucial genes for maintaining intestinal macrophage cell homeostasis. This is also supported by the step of exosome formation in mammalian cells that consists of the fusion between the multivesicular bodies (MVBs) and the plasma membrane of cells and so allows the delivery of their microRNA content [37,38]. The fact that broccoli vesicles, which could behave like MVBs, were able to enter keratinocytes, which subsequently emitted fluorescence, suggests delivery of the encapsulated material. However, the fusion of vesicles with the keratinocyte membrane and/or endocytoses could have occurred.

In addition, the presence of aquaporins from *Brassica* in the keratinocyte culture provides further evidence for the interaction between membranes, and it explains the greater cell swelling observed when vesicles were added to the NHEK culture, due to the new aquaporin incorporation. The aquaporins (PIP2-4 and NIP4-2) identified have only 28% homology with AQP3, according to a protein blast analysis performed with AQP3 versus either PIP2-4 or NIP4-2 (data not shown). AQP3 is the main aquaporin localised in human skin [39], so the absence of homology with the plant aquaporins identified in this work allows us to establish that there were *Brassica* aquaporins in the plasma membrane of keratinocytes even after repeated washes and complete replacement of the keratinocyte medium. The fact that other plasma membrane proteins were found during identification indicates the specificity of the extraction method as well as the accuracy of the mass spectroscopy analysis. The most critical point could be the understanding of the internalisation of the plant vesicles into keratinocytes. From one side, the fact that plant aquaporins were found in the isolated total plasma membrane could be just because the plant vesicles were incorporated into keratinocytes via an endosomal pathway. From the other side, the keratinocytes showed higher water transport (swelling experiments) through their plasma membrane when broccoli vesicles were incorporated. But this point can also be explained by an increase in aquaporin expression of the keratinocytes, as has been reported for mice, in which after application of exosomes from several plant species, an induction of the expression of genes for an anti-inflammation cytokine was observed [36].

In skin therapies and cosmetics the encapsulated bioactive compounds must cross the SC to be effective, and that it is a limit-

ing step. By identifying FNA in the internal skin layers, our results indicate that broccoli vesicles crossed the SC. When FNA was encapsulated in the broccoli vesicles we could detect green fluorescence in the inner layers of the skin even though FNA has low permeability through the superficial layer of the skin [40]. Therefore, our vesicles were able to reach the inner skin layers. Also, in our experiments, the fact that fluorescence was found in the endodermis demonstrates that the tight junctions in the epidermis [6] are not a barrier for our vesicles. Similarly, Lademann *et al.* [41] investigated the follicular penetration depth of a topically applied dye (FNA) in particle and non-particle form nanoparticles (average diameter 320 nm, PDI 0.06). Therefore, our vesicles were effective nanocarriers that crossed the most superficial layer of skin and released the encapsulated compound into the skin cells. However, the fact that the average diameter of the broccoli vesicles was 361.28 nm and their average PDI was 0.29 indicates that a proportion of the vesicles (those ranging from 10 to 210 nm in diameter) would penetrate through the transfollicular route [27]. The penetrability results obtained may be applicable to a living human skin, because porcine skin is very similar to its human counterpart, both structurally and chemically [42]. Besides, porcine and human skin have a comparable SC thickness of 21–26 μm and it has been established that porcine skin is a suitable substitute for human skin, especially in studies of percutaneous penetration and diffusion of materials and drugs.

Finally, an important consideration for using a compound in cosmetics or therapies is the product's shelf-life. A study of the stability and functionality of broccoli vesicles in a formulation was carried out for 1 year. The cosmetic formula was water-based, with no oil present for skin hydration, and used sodium benzoate, potassium benzoate and citric acid as preservatives. The fact that the cosmetic contained glycerine, as the vesicles were diluted in glycerol, would have helped the maintenance of the surface tension of the vesicles in keratinocytes and in skin epidermis. In accordance with the provisions of Martínez-Ballesta *et al.* [19], *Pf* measurement is related to vesicle and aquaporin functionality and membrane integrity. Our results show that no significant changes in the *Pf* value of broccoli vesicles added to the formulation occurred over the course of 1 year. However, the amount of protein did decline during that time. Furthermore, the relationship of aquaporins with the lipid bilayer is complex but each mutually confers stability on the other in this natural system [11]. This fact could explain the similar *Pf* values obtained with time. However, the decrease in the amount of recovered protein in the cosmetic from 24 h to 1 month should be investigated in order to determine the optimal composition of the cosmetic. Also, the fact that the recovered vesicles had their original shape but showed greater variability in size (Fig. 6d) could be a consequence of the recovery process.

Conclusions

In summary, we have shown that vesicles derived from broccoli roots could serve as nanocarriers for drugs, by demonstrating their stability and their relatively high entrapment efficiency, delivery and penetrability in skin tissue. The results show interactions between plant and human cell membranes that could lead to many lines of investigation and numerous potential applications. In fact, nanotechnology with vesicles obtained from plants could constitute a very promising area due to their low toxicity and their similarities to membranes from animal cells.

Compliance with ethics requirements

This article does not contain any studies with human or animal subjects.

CRedit authorship contribution statement

Lucía Yepes-Molina: Investigation, Methodology, Writing - original draft. **Maria Carmen Martínez-Ballesta:** Conceptualization, Investigation, Methodology, Validation, Writing - original draft. **Micaela Carvajal:** Conceptualization, Funding acquisition, Investigation, Methodology, Supervision, Validation, Writing - original draft.

Declaration of Competing Interest

The authors declare that they have no known competing financial interests or personal relationships that could have appeared to influence the work reported in this paper.

Acknowledgements

This work was funded by the Spanish Ministerio de Economía, Industria y Competitividad (AGL2016-80247-C2-1-R). The authors thank Sakata Seed Iberica S.L.U. for providing the broccoli seeds. The authors thank Provital S.A. for providing the formulation used in the experiment determining vesicle stability.

Appendix A. Supplementary material

Supplementary data to this article can be found online at <https://doi.org/10.1016/j.jare.2020.02.004>.

References

- [1] Danafar H, Shara fi A, Askarlou S, Manjili HK. Preparation and characterization of PEGylated iron oxide-gold nanoparticles for delivery of sulforaphane and curcumin. *Drug Res (Stuttg)* 2017;67:698–704. <https://doi.org/10.1055/s-0043-115905>.
- [2] Nounou MI, El-Khordagui LK, Khalafallah NA, Khalil SA. Liposomal formulation for dermal and transdermal drug delivery: past, present and future. *Recent Pat Drug Deliv Formul* 2008;2:9–18. <https://doi.org/10.2174/187221108783331375>.
- [3] Roberts MS, Cross SE, Pellett MA. Skin transport. *Dermatol Transderm Formul* 2002;89–196.
- [4] Bos JD, Meinardi MMHM. The 500 Dalton rule for the skin penetration of chemical compounds and drugs. *Exp Dermatol* 2000;9:165–9. <https://doi.org/10.1034/j.1600-0625.2000.009003165.x>.
- [5] Piérard GE, Courtois J, Ritacco C, Humbert P, Fanian F, Piérard-Franchimont C. From observational to analytical morphology of the stratum corneum: progress avoiding hazardous animal and human testings. *Clin Cosmet Investig Dermatol* 2015;8:113–25. <https://doi.org/10.2147/CCID.S77027>.
- [6] Andrews SN, Jeong E, Prausnitz MR. Transdermal delivery of molecules is limited by full epidermis, not just stratum corneum. *Pharm Res* 2013;30:1099–109. <https://doi.org/10.1007/s11095-012-0946-7>.
- [7] Shim J, Kang HS, Park WS, Han SH, Kim J, Chang IS. Transdermal delivery of mixnoxidil with block copolymer nanoparticles. *J Control Release* 2004;97:477–84. <https://doi.org/10.1016/j.jconrel.2004.03.028>.
- [8] Kanikkannan N, Singh M. Skin permeation enhancement effect and skin irritation of saturated fatty alcohols. *Int J Pharm* 2002;248:219–28. [https://doi.org/10.1016/S0378-5173\(02\)00454-4](https://doi.org/10.1016/S0378-5173(02)00454-4).
- [9] Souto EB, Müller RH. Cosmetic features and applications of lipid nanoparticles (SLN[®], NLC[®]). *Int J Cosmet Sci* 2008;30:157–65. <https://doi.org/10.1111/j.1468-2494.2008.00433.x>.
- [10] Seneviratne R, Khan S, Moscrop E, Rappolt M, Muench SP, Jeuken LJC, et al. A reconstitution method for integral membrane proteins in hybrid lipid-polymer vesicles for enhanced functional durability. *Methods* 2018;147:142–9. <https://doi.org/10.1016/j.ymeth.2018.01.021>.
- [11] Martínez-Ballesta MC, Pérez-Sánchez H, Moreno DA, Carvajal M. Plant plasma membrane aquaporins in natural vesicles as potential stabilizers and carriers of glucosinolates. *Colloids Surf B Biointerf* 2016;143:318–26. <https://doi.org/10.1016/j.colsurfb.2016.03.056>.
- [12] Ju S, Mu J, Dokland T, Zhuang X, Wang Q, Jiang H, et al. Grape exosome-like nanoparticles induce intestinal stem cells and protect mice from DSS-induced colitis. *Mol Ther* 2013;21:1345–57. <https://doi.org/10.1038/mt.2013.64>.
- [13] Wang Q, Zhuang X, Mu J, Bin Deng Z, Jiang H, Xiang X, et al. Delivery of therapeutic agents by nanoparticles made of grapefruit-derived lipids. *Nat Commun* 2013;4. <https://doi.org/10.1038/ncomms2886>.
- [14] György B, Hung ME, Breakefield XO, Leonard JN. Therapeutic applications of extracellular vesicles: clinical promise and open questions. *Annu Rev Pharmacol Toxicol* 2015;55:439–64. <https://doi.org/10.1146/annurev-pharmtox-010814-124630>.
- [15] Lo Cicero A, Stahl PD, Raposo G. Extracellular vesicles shuffling intercellular messages: For good or for bad. *Curr Opin Cell Biol* 2015;35:69–77. <https://doi.org/10.1016/j.ccb.2015.04.013>.
- [16] An Q, Hückelhoven R, Kogel KH, van Bel AJE. Multivesicular bodies participate in a cell wall-associated defence response in barley leaves attacked by the pathogenic powdery mildew fungus. *Cell Microbiol* 2006;8:1009–19. <https://doi.org/10.1111/j.1462-5822.2006.00683.x>.
- [17] Chalbi N, Martínez-Ballesta MC, Ben Youssef N, Carvajal M. Intrinsic stability of Brassicaceae plasma membrane in relation to changes in proteins and lipids as a response to salinity. *J Plant Physiol* 2015;175:148–56. <https://doi.org/10.1016/j.jplph.2014.12.003>.
- [18] Silva C, Aranda FJF, Ortiz A, Carvajal M, Martínez V, Teruel JAJA. Root plasma membrane lipid changes in relation to water transport in pepper: a response to NaCl and CaCl₂ treatment. *J Plant Biol* 2007;50:650–7. <https://doi.org/10.1007/bf03030609>.
- [19] Martínez-Ballesta M del C, García-Gómez P, Yepes-Molina L, Guarnizo AL, Teruel JA, Carvajal M. Plasma membrane aquaporins mediate vesicle stability in broccoli. *PLoS One* 2018;13:1–19. 10.1371/journal.pone.0192422.
- [20] Casado-Vela J, Muries B, Carvajal M, Iloro I, Elortza F, Martínez-Ballesta MC. Analysis of root plasma membrane aquaporins from brassica oleracea: Post-translational modifications, de novo sequencing and detection of isoforms by high resolution mass spectrometry. *J Proteome Res* 2010;9:3479–94. <https://doi.org/10.1021/pr901150g>.
- [21] Gekko K, Timasheff SN. Mechanism of protein stabilization by glycerol: preferential hydration in glycerol-water mixtures. *Biochemistry* 1981;20:4667–76. <https://doi.org/10.1021/bj00519a023>.
- [22] Mikami K, Katagiri T, Luchi S, Yamaguchi-Shinozaki K, Shinozaki K. A gene encoding phosphatidylinositol-4-phosphate 5-kinase is induced by water stress and abscisic acid in arabidopsis thaliana. *Plant J* 1998;15:563–8. <https://doi.org/10.1046/j.1365-313X.1998.00227.x>.
- [23] Ross DD, Joneckis CC, Ordóñez JV, Sisk AM, Wu RK, Hamburger AW, et al. Estimation of cell survival by flow cytometric quantification of fluorescein diacetate/propidium iodide viable cell number. *Cancer Res* 1989;49:3776–82.
- [24] Tian T, Zhu YL, Hu FH, Wang YY, Huang NP, Xiao ZD. Dynamics of exosome internalization and trafficking. *J Cell Physiol* 2013;228:1487–95. <https://doi.org/10.1002/jcp.24304>.
- [25] Tarhini M, Greige-Gerges H, Elaissari A. Protein-based nanoparticles: From preparation to encapsulation of active molecules. *Int J Pharm* 2017;522:172–97. <https://doi.org/10.1016/j.ijpharm.2017.01.067>.
- [26] Larsson C, Widell S, Kjellbom P. Preparation of high-purity plasma membranes. *Methods Enzymol* 1987;148:558–68. [https://doi.org/10.1016/0076-6879\(87\)48054-3](https://doi.org/10.1016/0076-6879(87)48054-3).
- [27] Danaei M, Dehghankhold M, Ataei S, Hasanzadeh Davarani F, Javanmard R, Dokhani A, et al. Impact of particle size and polydispersity index on the clinical applications of lipidic nanocarrier systems. *Pharmaceutics* 2018;10:57. <https://doi.org/10.3390/pharmaceutics10020057>.
- [28] Pávaióiu R-D, Sha'at F, Bubueanu C, Deaconu M, Neagu G, Sha'at M, et al. Polyphenolic Extract from Sambucus ebulus L. Leaves Free and Loaded into Lipid Vesicles. *Nanomaterials* 2019;10:56. 10.3390/nano10010056.
- [29] Ursache R, Andersen TG, Marhavý P, Geldner N. A protocol for combining fluorescent proteins with histological stains for diverse cell wall components. *Plant J* 2018;93:399–412. <https://doi.org/10.1111/tpi.13784>.
- [30] Flores R. A rapid and reproducible assay for quantitative estimation of proteins using bromophenol blue. *Anal Biochem* 1978;88:605–11. 10.1016/0003-2697(78)90462-1.
- [31] Ong SGM, Ming LC, Lee KS, Yuen KH. Influence of the encapsulation efficiency and size of liposome on the oral bioavailability of griseofulvin-loaded liposomes. *Pharmaceutics* 2016;8. 10.3390/pharmaceutics8030025.
- [32] Nii T, Ishii F. Encapsulation efficiency of water-soluble and insoluble drugs in liposomes prepared by the microencapsulation vesicle method. *Int J Pharm* 2005;298:198–205. <https://doi.org/10.1016/j.ijpharm.2005.04.029>.
- [33] Zhang M, Viennois E, Xu C, Merlin D. Plant derived edible nanoparticles as a new therapeutic approach against diseases. *Tissue Barriers* 2016;4. <https://doi.org/10.1080/21688370.2015.1134415e1134415>.
- [34] Bätz FM, Klipper W, Korting HC, Henkler F, Landsiedel R, Luch A, et al. Esterase activity in excised and reconstructed human skin – Biotransformation of prednicarbate and the model dye fluorescein diacetate. *Eur J Pharm Biopharm* 2013;84:374–85. <https://doi.org/10.1016/j.ejpb.2012.11.008>.
- [35] Yang Y, Wang J, Shigematsu H, Xu W, Shih WM, Rothman JE, et al. Self-assembly of size-controlled liposomes on DNA nanotemplates. *Nat Chem* 2016;8:476–83. <https://doi.org/10.1038/nchem.2472>.
- [36] Mu J, Zhuang X, Wang Q, Jiang H, Bin Deng Z, Wang B, et al. Interspecies communication between plant and mouse gut host cells through edible plant derived exosome-like nanoparticles. *Mol Nutr Food Res* 2014;58:1561–73. <https://doi.org/10.1002/mnfr.201300729>.
- [37] Lakhil S, Wood MJA. Exosome nanotechnology: An emerging paradigm shift in drug delivery: exploitation of exosome nanovesicles for systemic in vivo delivery of RNAi heralds new horizons for drug delivery across biological barriers. *BioEssays* 2011;33:737–41. <https://doi.org/10.1002/bies.201100076>.
- [38] An Q, van Bel AJ, Hückelhoven R. Do plant cells secrete exosomes derived from multivesicular bodies?. *Plant Signal Behav* 2007;2:4–7. <https://doi.org/10.4161/psb.2.1.3596>.
- [39] Qin H, Zheng X, Zhong X, Shetty AK, Elias PM, Bollag WB. Aquaporin-3 in keratinocytes and skin: its role and interaction with phospholipase D2. *Arch*

- Biochem Biophys 2011;508:138–43. <https://doi.org/10.1016/j.abb.2011.01.014>.
- [40] Coderch L, de Pera M, Perez-Cullell N, Estelrich J, de la Maza A, Parra JL. The effect of liposomes on skin barrier. *Structure* 1999;12:235–46.
- [41] Lademann J, Richter H, Teichmann A, Otberg N, Blume-Peytavi U, Luengo J, et al. Nanoparticles – an efficient carrier for drug delivery into the hair follicles. *Eur J Pharm Biopharm* 2007;66:159–64. <https://doi.org/10.1016/j.ejpb.2006.10.019>.
- [42] Kong R, Bhargava R. Characterization of porcine skin as a model for human skin studies using infrared spectroscopic imaging. *Analyst* 2011;136:2359–66. <https://doi.org/10.1039/c1an15111h>.